Observation of Dirac Cone Electronic Dispersion in $BaFe_2As_2$

P. Richard,[1,*] K. Nakayama,[2] T. Sato,[2,3] M. Neupane,[4] Y.-M. Xu,[4] J. H. Bowen,[5] G. F. Chen,[5] J. L. Luo,[5] N. L. Wang,[5] X. Dai,[5] Z. Fang,[5] H. Ding,[5] and T. Takahashi[1,2]

[1]*WPI Research Center, Advanced Institute for Materials Research, Tohoku University, Sendai 980-8577, Japan*
[2]*Department of Physics, Tohoku University, Sendai 980-8578, Japan*
[3]*TRiP, Japan Science and Technology Agency (JST), Kawaguchi 332-0012, Japan*
[4]*Department of Physics, Boston College, Chestnut Hill, Massachusetts 02467, USA*
[5]*Beijing National Laboratory for Condensed Matter Physics, and Institute of Physics, Chinese Academy of Sciences, Beijing 100190, China*

(Received 3 September 2009; revised manuscript received 17 December 2009; published 29 March 2010)

We performed an angle-resolved photoemission spectroscopy study of $BaFe_2As_2$, which is the parent compound of the so-called 122 phase of the iron-pnictide high-temperature superconductors. We reveal the existence of a Dirac cone in the electronic structure of this material below the spin-density-wave temperature, which is responsible for small spots of high photoemission intensity at the Fermi level. Our analysis suggests that the cone is slightly anisotropic and its apex is located very near the Fermi level, leading to tiny Fermi surface pockets. The bands forming the cone show an anisotropic leading edge gap away from the cone that suggests a nodal spin-density-wave description.

DOI: 10.1103/PhysRevLett.104.137001 PACS numbers: 74.70.−b, 71.18.+y, 74.25.Jb, 79.60.−i

As with cuprates, it is widely believed that high-T_c superconductivity in pnictides emerges by tuning interactions already present in the parent compounds. For example, high-T_c superconductivity up to 37 K is achieved in metallic and antiferromagnetic $BaFe_2As_2$ by adding carriers [1,2] or applying pressure [3,4]. Although long-range magnetic order is suppressed at optimal T_c, previous angle-resolved photoemission spectroscopy (ARPES) [5,6] and neutron scattering studies [7] strongly suggest the importance of magnetic fluctuations for the pairing mechanism. While it is admitted that the parent compounds $BaFe_2As_2$, $SrFe_2As_2$, and $CaFe_2As_2$ exhibit a magnetic ordering below a spin-density-wave (SDW) transition temperature T_{SDW} that is accompanied by an orthorhombic distortion [8–10], the nature of the force driving this transition remains controversial.

Owing to its angle-resolved capability to measure directly single-particle electronic spectra, ARPES is a powerful tool that allows a precise description of the Fermi surface (FS) topology and the electronic states lying in the vicinity of the Fermi level (E_F). However, previous attempts by ARPES to elucidate the nature of the low-temperature (T) electronic states of the pnictide parent compounds support competing scenarios, including SDW [11] and exchange splitting [12] models. Even more challenging is to answer whether the signatures of tiny FSs inferred from quantum oscillation experiments (QOE) [13,14], which cannot be experimentally located in the momentum space, are analogous to the FS reconstructions claimed in cuprates [15] or are consequences of more fundamental topological anomalies in the electronic structure, such as the Dirac cone in graphene [16]. It is thus imperative to characterize directly and more precisely the electronic states that trigger the low-T properties of the pnictide parent compounds.

In this Letter, we report an ARPES investigation of the low-energy electronic states of $BaFe_2As_2$. We show that low-T $BaFe_2As_2$ is better described as a nodal SDW system [17]. We reveal an anisotropic Dirac cone located away from high-symmetry points and formed by bands that are gapped away from the cone. The cone's apex is located very near E_F, which implies tiny FS pockets.

High-quality single crystals of $BaFe_2As_2$ ($T_{SDW} = 138$ K) have been grown using the flux method [1]. A microwave-driven helium source ($h\nu = 21.218$ eV) and a VG-Scienta SES 2002 multichannel analyzer were used to record ARPES spectra with energy and angular resolutions of 7–14 meV and 0.2°, respectively. The samples were cleaved *in situ* at 25 K and measured with a working vacuum better than 5×10^{-11} Torr within the 25–170 K T range. No obvious degradation of the spectra was observed for typical measurements of 3 days. A freshly evaporated gold sample in electrical contact with the $BaFe_2As_2$ sample served to calibrate E_F. To facilitate data representation, we describe all the results in terms of the unreconstructed Brillouin zone (BZ) formed by the Fe network alone, with the lattice parameter a representing the distance between Fe atoms.

In Fig. 1(a), we show a FS mapping obtained at 25 K. Two regions of similar size with high intensity are centered around the zone center (Γ point) and the $M(\pi, 0)$ point [(π, π) in the reconstructed BZ], respectively. The main focus of this Letter is a very bright spot observed around $(0.75\pi, 0)$ on the Γ-M symmetry line. The second derivative intensity plot of the FS shown in Fig. 1(b) suggests that the FS is folded across the 2D low-T BZ and that the Γ- and

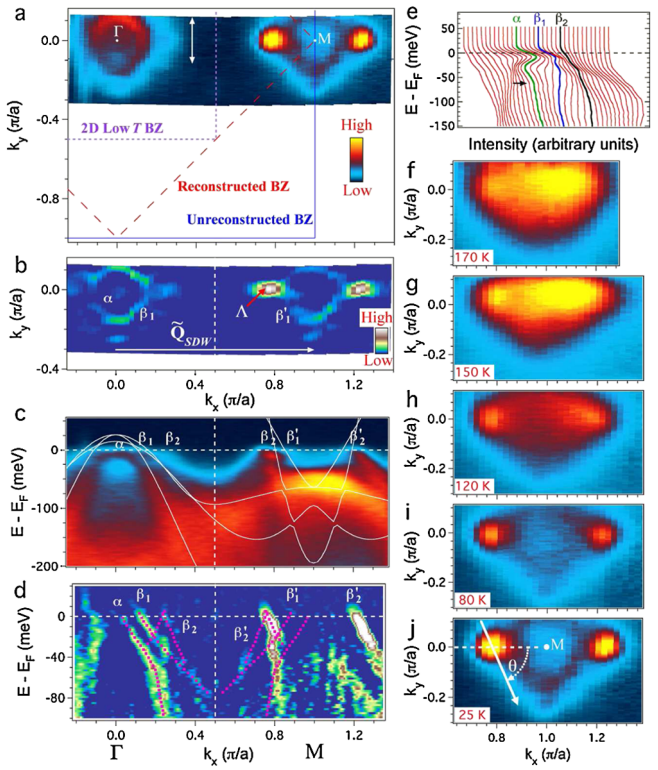

FIG. 1 (color online). (a) FS mapping (25 K) obtained by integrating the photoemission intensity in a 20 meV window centered at E_F. The FS is described in terms of the unreconstructed BZ. The double arrow indicates light polarization. (b) Corresponding second derivative intensity plot. $\tilde{Q}_{\mathrm{SDW}}$ is the in-plane projection of the SDW wave vector. (c),(d) ARPES intensity plot and corresponding second momentum derivative intensity plot, respectively, along the $\Gamma(0, 0)$-$M(\pi, 0)$ symmetry line. The dotted lines are guides for the eye. The solid lines in (c) correspond to our LDA calculated bands renormalized by a factor of 3. The vertical dashed lines in (b)–(d) indicate the 2D low-T BZ. (e) EDCs around Γ. The arrow indicates the bottom of an e-like dispersion that hybridizes with the α and β_1 bands. (f)–(j) T evolution of the FS around M. The angle θ is defined in (j).

M-centered FSs are replica connected by the $\tilde{Q}_{\mathrm{SDW}} = (\pi, 0)$ wave vector [(π, π) in the reconstructed BZ description]. This is clear for the β_1 FS and its reflection β_1', as well as for the bright spot and its equivalent symmetry points $(\pm 0.25\pi, 0)$. Unfortunately, we cannot conclude whether the fourfold symmetric FS pattern observed around the Γ and M points is intrinsic or due to the superimposition of twin domains expected to form below T_{SDW}, where an orthorhombic distortion and an orthorhombic magnetic structure take place [8–10].

The intensity plot of the Γ-M cut is given in Fig. 1(c), and the corresponding second momentum derivative intensity plot (2MIP) is displayed in Fig. 1(d). Even after renormalization by a factor of 3 for a better correspondence with the gross experimental features, neither our local-density approximation (LDA) calculations in the paramagnetic state displayed in Fig. 1(c) nor others found in literature [18,19] can be successfully folded across the 2D low-T BZ boundary to account for a perfect description of all bands and especially for the small intensity spot at the Λ point. In addition to the α and β_1 bands expected from a comparison with optimally doped samples [5], an extra holelike (h-like) dispersion crossing E_F (β_2) below T_{SDW} is observed around the Γ point, in agreement with previous reports on $BaFe_2As_2$ [12] and $CaFe_2As_2$ [20]. This band is also folded across the 2D low-T BZ boundary. It crosses E_F at $\Lambda = (0.75\pi, 0)$, which corresponds to the bright spot. The T evolution of the FS, displayed in Figs. 1(f)–1(j), indicates that while the bright spot at the Λ point is clearly visible up to 120 K, it becomes hard to identify at 150 K and above, reinforcing our assumption that the spot at the Λ point is formed, at least partly, by an extra band that appears below T_{SDW} (138 K). Interestingly, an electronlike (e-like) band crosses E_F at the same point. As expected, the energy distribution curves (EDCs) given in Fig. 1(e) show that this band is folded to the Γ point. Moreover, it hybridizes with both the α and β_1 bands, opening energy gaps below E_F.

One question immediately follows: Does that e-like band hybridize with the β_2' band around the Λ point as well? To answer and characterize the Λ point further, we plot in the top row of Fig. 2 cuts going through the Λ point and indexed according to the θ angle defined in Fig. 1(j). The corresponding second energy derivative intensity plots (2EIPs) and 2MIPs are displayed in the second and third rows of Fig. 2, respectively. They exhibit a complicated hybridization pattern. For instance, the hybridization between the e-like band and the β_1' at $\theta = 0$ manifests itself by a gap in the 2EIP in the ~20–30 meV binding energy range and close to a vertical section of the dispersion for the same energy range in the 2MIP.

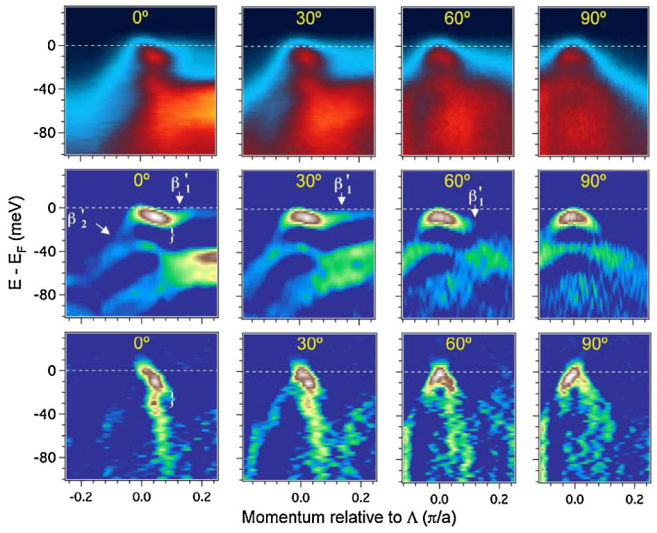

FIG. 2 (color online). ARPES intensity plots (25 K) for cuts going trough $\Lambda(075\pi, 0)$ are displayed in the top row and indexed after the θ angle defined in Fig. 1(j). The corresponding 2EIPs and 2MIPs are shown in the second and third rows, respectively. The direction of the straight arrow in Fig. 1(j) defines the momentum increase, which is towards M for $\theta = 0$.

Surprisingly, the portion of the band structure around the Λ point, from E_F to a binding energy of about 20 meV, seems not to change much with θ: an *e*-like band and an *h*-like band intersect around E_F and their angular symmetry defines a cone structure, well illustrated by the angular evolution of the 2MIPs, which are not distorted by the Fermi edge [21]. By dividing a spectra recorded at 100 K ($<T_{SDW}$) by the Fermi-Dirac function convoluted with the instrumental resolution [Fig. 3(a)], we can partly access the electronic band structure above E_F. Despite thermal broadening, the resulting intensity plot and its 2MIP displayed in Fig. 3(b) clearly show the *X*-like structure of a Dirac cone. This result contradicts a report attributing the Λ spot to the top of a *h*-like band instead of a Dirac cone, despite the resemblance [22]. The EDCs around the Λ point given in Fig. 3(b) suggest the absence of hybridization gap at the Λ point, at least within our resolution. Hereafter, we thus refer to this structure as a Dirac cone, as observed in graphene [16].

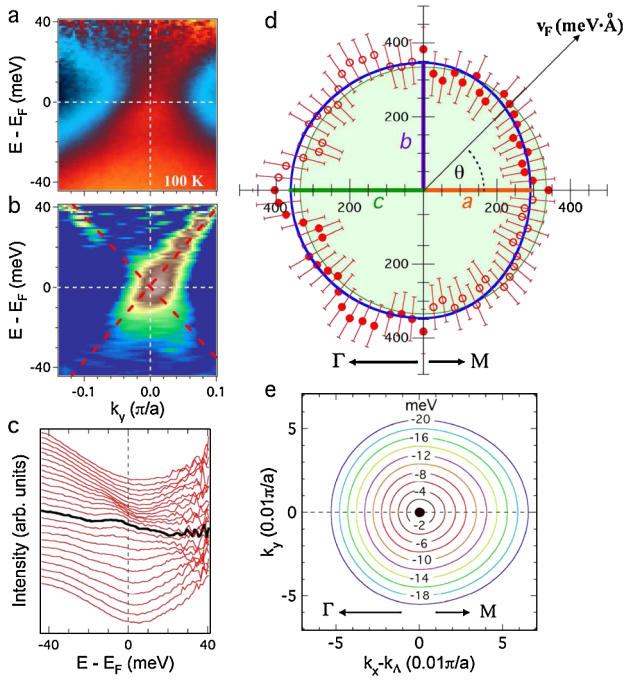

FIG. 3 (color online). (a) ARPES intensity spectra of $BaFe_2As_2$ at the Λ point ($\theta \sim 90°$) recorded at 100 K, after division by the Fermi-Dirac function convoluted with the instrumental resolution function. (b) Corresponding 2MIP. Long dashed lines are guides for the eye. The corresponding EDCs are given in (c), where the bold EDC refers to the Λ point. (d) Polar representation of v_F around the Λ point (25 K). Open circles and closed circles represent data measured and data obtained by reflection with respect to the Γ-*M* symmetry line, respectively. The large filled circle represents the average value of v_F while the thick line is a fit of the data to the two-ellipse model described in the text, with parameters *a*, *b*, and *c*. (e) Contour plot of the electronic dispersion below E_F around the Λ point, as calculated from our model. The small filled circle represents the FS associated with the cone.

Unlike the high-symmetry location of isotropic Dirac cone in graphene, the Λ point in $BaFe_2As_2$ is not a high-symmetry point. To investigate the possible anisotropy of the band structure around Λ, we extracted the Fermi velocity (v_F) as a function of θ by assuming a linear dispersion in the vicinity of E_F. The data are reported on a polar plot in Fig. 3(d). The size of the plain circle represents the 330 ± 60 meV · Å average of v_F. Although it is consistent with the data within uncertainties, a better agreement is achieved if we assume a small anisotropy. Since symmetry across the Γ-*M* axis is the only constraint imposed at the Λ point, we fitted the data with two ellipses defined by half-axes (*a, b*) and (*c, b*), respectively, the *b* axis being perpendicular to the Γ-*M* direction, i.e., for $\theta = \pm 90°$. As illustrated in Fig. 3(c), we obtained $v_F(a) = 290 \pm 60$ meV · Å, $v_F(b) = 350 \pm 60$ meV · Å, and $v_F(c) = 360 \pm 60$ meV · Å, respectively.

Our analysis reveals that the apex of the cone is located 1 ± 5 meV above E_F, which corresponds to E_F within uncertainties. Figure 3(e) shows a contour plot of the cone dispersion below E_F reconstructed by assuming a linear dispersion, a cone apex located 1 meV above E_F, and v_F values derived from the *a*, *b*, and *c* parameters. With the cone apex located 1 meV above E_F, the FS size, which corresponds to the small filled surface in Fig. 3(e), is only 1×10^{-3}% of the reconstructed BZ, a value smaller than the estimation obtained from QOE in $SrFe_2As_2$ [13] and $BaFe_2As_2$ [14]. However, the FS size is very sensitive to the position of E_F. While a downward chemical potential shift of 8 meV would lead to an area of 1% of the reconstructed BZ similar to the values reported by QOE [13,14], an upward shift of only slightly more than 1 meV would switch the FS from *h*-like to *e*-like. In Fig. 4(a), we plot a 3D representation of the anisotropic Dirac cone in the vicinity of E_F calculated from our model.

What physical mechanism can generate such a topological anomaly in the electronic band structure and the FS of $BaFe_2As_2$? Within the framework of SDW mean-field theory of both two-band and five-band tight-binding models, Ran *et al.* demonstrated that nodes in the SDW gap function of undoped FeAs-based superconductors must exist due to the occurrence of Dirac cones forming as a consequence of the symmetry-enforced degeneracy at the Γ and *M* high-symmetry points, even in the presence of perfect nesting [17]. These nodes are located in the same region as the cone that we observe. The gap function is predicted to vary away from the cone. We investigated this scenario by measuring the leading edge gap (LEG) of EDCs at the minimum gap locus (MGL) on cuts around the *M* point. For this, we define the angle ω in Fig. 4(b) and display the results in Fig. 4(c). As ω increases, the LEG shifts towards high binding energy. The peak is also suppressed and the MGL is ill-defined above 25°, leading to large uncertainties in the value of the LEG (ω) given in the inset of Fig. 4(c). We also note that the LEG at $\omega = 0$ is located 3.5 meV above E_F, and thus we shifted LEG (ω) by that value.

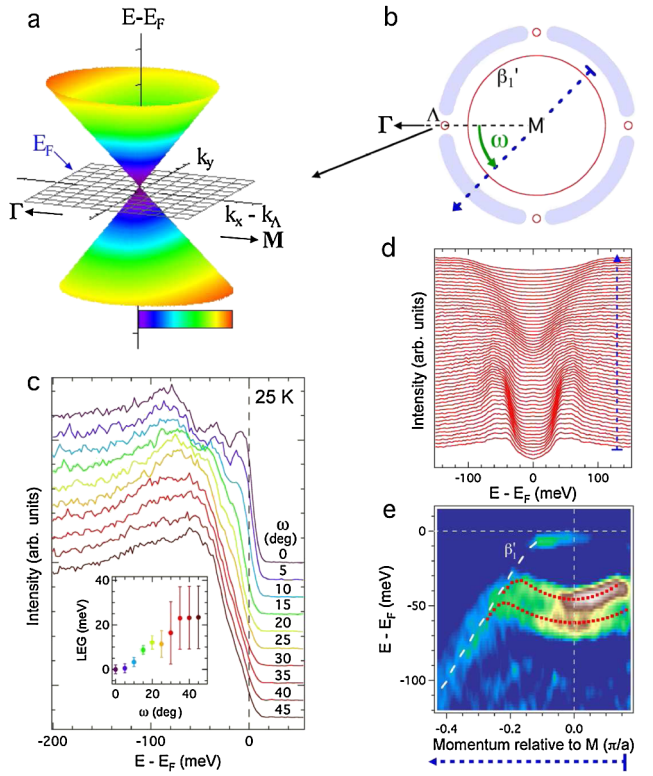

FIG. 4 (color online). (a) 3D representation of the Dirac cone at Λ. The color scale indicates the distance from Λ. (b) Schematic FS around the M point. The folded α band, which is barely touching E_F, is not indicated. Shaded areas indicate gapped regions and the dashed arrow indicates the orientation of the ARPES cut associated with (d) and (e). (c) MGL of EDCs (25 K) as a function of the angle ω defined in (b). The inset shows the LEG as a function of ω after a 3.5 meV shift (see the text). (d) Symmetrized EDCs (25 K) along the cut indicated in (b). (e) 2EIP (25 K) along the cut indicated in (b). The vertical dashed line indicates the M point.

Even though the MGL of the bands forming the Dirac cone is uncertain for large ω, both the symmetrized EDCs [Fig. 4(d)] and the 2EIP [Fig. 4(e)] corresponding to the cut indicated by a dashed arrow in Fig. 4(b) suggest that they are gapped. In fact, as supported by the 2EIP given in Fig. 4(e), two e-like bands exhibit gaps of ~50 and ~30 meV. Since the apex of the cone is located approximately at E_F, it is a good first approximation to assume that SDW gaps is centered near E_F as well. Our results would correspond to full SDW gaps of ~100 and ~60 meV, respectively. Although further studies are necessary to conclude that these gap values correspond to optical gaps, it is remarkable that they agree reasonably well with the 110 and 45 meV gaps reported from optical measurements on $BaFe_2As_2$ single crystals [23].

We caution that we did not consider k_z dispersion [20,24,25]. Although the α band has a strong k_z dependence, Liu *et al.* reported only little variations for the β_1 and β_2 bands [20]. The latter, which coincides with the Λ point, is found around both the Γ and M points, confirming band folding. Because of the sensitivity of the Dirac cone apex position to the precise e-like and h-like dispersions generating the cone, it is likely that even a very small wiggling in the k_z dispersion can lead to a shift of the cone apex and produce the series of very small FSs suggested from QOE [13,14]. Even though the failure of QOE to detect the large h-like β_1 FS pocket observed by ARPES and predicted by calculations remains puzzling, our observation of tiny FSs in the parent compound of an iron-pnictide superconductor derived from a fundamental topological anomaly, i.e., a Dirac cone dispersion, is of crucial importance to understand the unconventional electronic properties of these materials and allows us to describe them as nodal SDW materials.

We thank Z. Wang and S. Zhou for valuable discussions. This work was supported by grants from JSPS, JST-TRIP, JST-CREST, MEXT of Japan, the Chinese Academy of Sciences, Ministry of Science and Technology of China, and NSF of the U.S.

Note added—After completion of our work, we became aware of a QOE study confirming the values of v_F determined in this work and supporting the present set of data [26].

*p.richard@arpes.phys.tohoku.ac.jp

[1] G. F. Chen *et al.*, Phys. Rev. B **78**, 224512 (2008).
[2] M. Rotter, M. Tegel, and D. Johrendt, Phys. Rev. Lett. **101**, 107006 (2008).
[3] S. A. J. Kimber *et al.*, Nature Mater. **8**, 471 (2009).
[4] M. S. Torikachvili *et al.*, Phys. Rev. B **78**, 104527 (2008).
[5] H. Ding *et al.*, Europhys. Lett. **83**, 47001 (2008).
[6] P. Richard *et al.*, Phys. Rev. Lett. **102**, 047003 (2009).
[7] A. D. Christianson *et al.*, Nature (London) **456**, 930 (2008).
[8] Q. Huang *et al.*, Phys. Rev. Lett. **101**, 257003 (2008).
[9] J. Zhao *et al.*, Phys. Rev. Lett. **101**, 167203 (2008).
[10] S. D. Wilson *et al.*, Phys. Rev. B **79**, 184519 (2009).
[11] D. Hsieh *et al.*, arXiv:0812.2289v1.
[12] L. X. Yang *et al.*, Phys. Rev. Lett. **102**, 107002 (2009).
[13] S. E. Sebastian *et al.*, J. Phys. Condens. Matter **20**, 422203 (2008).
[14] J. G. Analytis *et al.*, Phys. Rev. B **80**, 064507 (2009).
[15] N. Doiron-Leyraud *et al.*, Nature (London) **447**, 565 (2007).
[16] K. S. Novoselov *et al.*, Nature (London) **438**, 197 (2005).
[17] Y. Ran *et al.*, Phys. Rev. B **79**, 014505 (2009).
[18] C. Liu *et al.*, Phys. Rev. Lett. **101**, 177005 (2008).
[19] D. J. Singh, Phys. Rev. B **78**, 094511 (2008).
[20] C. Liu *et al.*, Phys. Rev. Lett. **102**, 167004 (2009).
[21] An azimuthal symmetry around Λ is observed down to higher binding energies, but we focused our analysis near E_F to avoid regions where hybridization is observed.
[22] G. Liu *et al.*, Phys. Rev. B **80**, 134519 (2009).
[23] W. Z. Hu *et al.*, Phys. Rev. Lett. **101**, 257005 (2008).
[24] P. Vilmercati *et al.*, Phys. Rev. B **79**, 220503(R) (2009).
[25] W. Malaeb *et al.*, J. Phys. Soc. Jpn. **78**, 123706 (2009).
[26] N. Harrison and S. E. Sebastian, Phys. Rev. B **80**, 224512 (2009).